Annals of the Entomological Society of America, 118(4), 2025, 315–330
https://doi.org/10.1093/aesa/saaf019
Advance Access Publication Date: 3 July 2025
Research

ENTOMOLOGICAL SOCIETY OF AMERICA
SHARING INSECT SCIENCE GLOBALLY

OXFORD

Research

Description of a new species of subterranean termite in the genus *Reticulitermes* (Blattodea: Heterotermitidae) from southern California

Joanne Tzu-Chia Chen[1], Lori Nelson[2], Paul F. Rugman-Jones[1], Shu-Ping Tseng[3], Andrew M. Sutherland[4], Dong-Hwan Choe[1], Michael I. Haverty[2], and Chow-Yang Lee[1,*]

[1]Department of Entomology, University of California, Riverside, CA, USA
[2]USDA Forest Service, Pacific Southwest Research Station, Vallejo, CA, USA
[3]Department of Entomology, National Taiwan University, Taipei, Taiwan
[4]Division of Agriculture and Natural Resources, University of California, Hayward, CA, USA

[*]Corresponding author. Department of Entomology, University of California, 900 University Ave. Riverside, CA 92521, USA (Email: chowyang.lee@ucr.edu).

Subject Editor: Kathleen Walker

Received on 19 February 2025; revised on 28 April 2025; accepted on 7 May 2025

Using morphological assessments and phylogenetic inference, we described a new subterranean termite species in the genus *Reticulitermes* in southern California: *Reticulitermes rusti* sp. nov. Genetic analyses utilizing 3 mitochondrial loci (*16S rRNA*, *COI*, and *COII*) and 7 microsatellites successfully distinguished the new species from 2 other *Reticulitermes* found in southern California: *R. hesperus* Banks and *R. tibialis* Banks. Empirical measurements of key morphological characters further support the delineation of *R. rusti* as a new species. While *R. rusti* is genetically closer to *R. tibialis*, its soldier caste is morphologically similar to that of *R. hesperus*. We recommend confirming species identification by sequencing the COI or COII region. The integration of biological, genetic, and morphological data robustly supports the recognition of *R. rusti* as a distinct new species in southern California.

Keywords: structural pest, COI, COII, 16S rRNA, microsatellites, integrative taxonomy

Introduction

The taxonomy of *Reticulitermes* in California has been a subject of ongoing debate. Early studies on Californian termites suggested that only 2 species were present: *R. hesperus* Banks and *R. tibialis* Banks (Light and Pickens 1934, Pickens 1934, Snyder 1949, 1954). However, more recent profiling of the cuticular hydrocarbons (CHCs) of *Reticulitermes* from northern California revealed 5 distinct CHC phenotypes, suggesting the presence of additional species (Haverty and Nelson 1997). Following this discovery, further evidence supporting the existence of potentially undescribed species of *Reticulitermes* has accumulated from studies utilizing CHC profiles (Nelson et al. 2001, 2008, 2022, Copren et al. 2005, Haverty and Nelson 2007), soldier defense secretion profiles (Nelson et al. 2001, 2008), flight phenology comparisons (Haverty et al. 2003), behavior (Haverty et al. 1999, Delphia et al. 2003), and phylogenetic approaches (Copren et al. 2005, Su et al. 2006, Tseng et al. 2023). Nelson et al. (2008) suggested the presence of at least 7 *Reticulitermes* species in California. These include the described species *R. hesperus*, *R. tibialis*, and *R. flavipes* (Kollar) (Su et al. 2006), as well as 4 potentially undescribed species (Nelson et al. 2008).

Phylogenetic studies of *Reticulitermes* species in California have primarily focused on 2 mitochondrial DNA loci: COII (Copren et al. 2005) and/or 16S rRNA (Austin et al. 2005, Tripodi et al. 2006). With the increasing emphasis on systematics, phylogenetic approaches have increasingly complemented chemotaxonomic methods. Jenkins et al. (2000) were the first to demonstrate concordant results between these approaches when

examining *Reticulitermes* species in the southeastern United States. In California, a correlation between CHC phenotypes and mtDNA COII variation was identified by Copren et al. (2005), further demonstrating the utility of both methods for *Reticulitermes* identification (Copren et al. 2005, Nelson et al. 2008). Tseng et al. (2023) incorporated nuclear DNA loci ITS1 and ITS2 to improve clade delineation. However, the incongruence between the tree constructed by mtDNA COII and the tree constructed by nuclear loci ITS1 and ITS2 potentially challenged the accuracy of mtDNA markers in delineating species boundaries. Widely distributed species can undergo historical isolation and then merge during later expansion, resulting in the coexistence of distinct mtDNA haplotypes (Després 2019). Considering the wide distribution of *R. hesperus* (Banks and Snyder 1920, Nelson et al. 2008), more evidence beyond mtDNA is required.

In terms of morphology, although diagnostic keys for termites in the United States have been published in several studies (Banks and Snyder 1920, Snyder 1954, Gleason and Koehler 1980, Nutting 1990, Scheffrahn and Su 1994), those that include *Reticulitermes* species from the western US are limited, namely only in Banks and Snyder (1920) and Nutting (1990). While several researchers have noted that the undescribed species are morphologically indistinguishable, empirical measurements have rarely been provided (Szalanski et al. 2006, Tripodi et al. 2006). Only Haverty and Nelson (1997) included a detailed morphological analysis, where they measured characters of the soldier caste of the 4 northern California CHC phenotypes CA-A, CA-B, CA-C, and CA-D; however, the morphometric measurements failed to discriminate those CHC phenotypes from each other, and all were diagnosed morphologically as *R. tibialis* (Haverty and Nelson 1997). Later, Copren et al. (2005) identified additional CHC phenotypes, SC-A, SC-B, and SC-B′, in southern California, but the morphology of these lineages was not examined.

Species delimitation is the process of defining species boundaries using empirical data. A common approach for identifying morphologically ambiguous species involves examining the geographic zones where their ranges overlap. By investigating their genetic clustering of lineages in sympatric and parapatric settings, researchers can assess whether these lineages are genetically distinct. Such analysis provides insights into the reproductive barriers that emerge as species diverge (Abbott et al. 2013, Adams et al. 2014, Singhal et al. 2018).

According to the tree reconstructed using 16S rRNA, COII, ITS1, and ITS2 in Tseng et al. (2023), a total of three *Reticulitermes* CHC phenotypes, SC-A, SC-B, and SC-B′, fell into 2 candidate species CA-A and SC-B in southern California. Tseng et al. (2023) confirmed CA-A as *R. hesperus*, which is broadly distributed along the west coast of North America. In contrast, SC-B has so far only been found in southern California. The distribution patterns suggest that *R. hesperus* may overlap with the ranges of the SC-B phenotype, providing an ideal area to examine if these phenotypes can be separated as a biological species.

The aim of this study is to reexamine the relationship between the SC-B phenotype and *R. hesperus* using samples collected in southern California. Our objectives were to (i) confirm the sympatric distribution of the CHC phenotype SC-B and *R. hesperus*, (ii) investigate genetic clustering among sympatric populations of these 2 lineages using 7 microsatellite markers, and (iii) assess morphological variation within and between the lineages through direct measurement. Finally, if all the evidence pointed SC-B as a distinct species, we shall propose it as a new species.

Materials and Methods

Sample Collection and Processing Procedures

Specimens of *Reticulitermes* used in this study were collected across California from 2005 to 2024. The collections primarily focused on locations in southern California; however, collections were made from Riverside to Monterey, CA. Termites were obtained either through direct field collection by the senior author and other coauthors, or from specimens collected and sent by pest management professionals (PMPs). The insects were primarily collected from decaying wood, tree stumps, twigs, fallen branches, and infested structures. Specimens containing soldier castes were mainly collected directly from wood sources in the field, while colonies with soldiers from University of California Riverside were collected using in-ground termite monitoring stations. Imagoes were collected during *Reticulitermes* swarming seasons, typically in fall/winter, and spring, either by the authors or with the assistance of PMPs. The number of individuals collected for each colony varied depending on the number of insects that were available during the collection. Whenever possible, we attempted to collect at least 50 workers per colony, along with as many soldiers and imagoes. Field-collected termites were preserved using 2 different methods: specimens intended for molecular analyses were stored in 100% ethanol, while those designated for morphological examination were kept in 75% ethanol.

For DNA extraction, one worker termite per colony was used. In situation when worker termites were absent, DNA was extracted from an alate. Morphometric measurements were performed on soldier or alate castes in colonies which the specimens were available. For those colonies, 1 to 5 soldiers and/or imagoes were measured. DNA samples from Tseng et al. (2023) were also included to amplify the cytochrome c oxidase subunit I (COI) region. Comprehensive details, including collection locations and sample characteristics, can be found in Table S1.

DNA Extraction

For each sample collected in this study, a single worker or alate was subjected to DNA extraction. The only exception was the *R. tibialis* colony (R066), which 8 workers were used and genotyped to allow inclusion in the PCA analysis. DNA extraction was performed using the Puregene Tissue Kit (Qiagen, Germany) following the "DNA Purification from Tissue" protocol outlined in the kit handbook (https://www.qiagen.com/us/Resources/ResourceDetail?id=a9e6a609-4600-4b03-afbd-974318590ce5&lang=en). The extracted DNA was dissolved in 200 µl of diethyl pyrocarbonate-treated water and stored at −20 °C for preservation. All DNA samples were first used for mtDNA sequence amplification. Samples with sufficient remaining DNA were subsequently used for microsatellite genotyping.

PCR Amplification and Sanger Sequencing

To obtain sequences from 16S rRNA, COI, and COII regions, DNA samples extracted in this study were used to amplify all 3 loci, while DNA samples from Tseng et al. (2023) were used only for COI amplification, as COII and 16S rRNA sequences were already available in GenBank. The COI gene was amplified using primers LCO1490 (5′-GGTCAACAAATCATAAAGATATTGG-3′) and HCO2198 (5′-TAAACTTCAGGGTGACCAAAAAATCA-3′) (Folmer et al. 1994). The COII gene was amplified using primers TL2-J-3037 (5′-ATGGCAGATTAGTGCAATGG-3′) and TK-N-3785 (5′-GTTTAAGAGACCAGTACTTG-3′) (Simon et al. 1994). For the 16S rRNA gene, primers LR-J-13007 (5′-TTACGCTGTTATCCCTAA-3′) (Kambhampati and Smith 1995)

and LR-N-13398 (5′-CGCCTGTTTATCAAAAACAT-3′) (Simon et al. 1994) were used. PCR mixtures consisted of 1 µl of template DNA, 0.2 µM of each primer, and 12.5 µl of EmeraldAmp GT PCR Master Mix (Takara Bio, Japan), with nuclease-free water added to a final volume of 25 µl per reaction. The PCR protocol included an initial denaturation at 95 °C for 10 min, followed by 35 cycles of denaturation at 95 °C for 30 s, annealing at gene-specific temperatures (COI: 45 °C; COII: 52 °C; 16S: 50 °C) for 30 s, and extension at 72 °C for 45 s. A final extension step was performed at 72 °C for 10 min to complete the amplification. Post-amplification, PCR products were purified using the ExoSAP-IT PCR Product Clean-Up Reagent (ThermoFisher Scientific, MA). The purified samples were then submitted to Retrogen Inc. (San Diego, CA) for Sanger sequencing on an Applied Biosystems DNA Analyzer 3730xl. Sequence data were trimmed using Sequencher 4.9 (GeneCodes). GenBank accession numbers for each locus (16S rRNA, COI, COII) are provided in Table S2.

Mitochondrial Differentiation and Phylogenetic Inference

To investigate the phylogenetic relationships of *Reticulitermes* collected in southern California, 16S rRNA, COI, and COII partial sequences were used to reconstruct a phylogenetic tree via maximum likelihood inference. Sequences generated in the current study were supplemented with COII and 16S rRNA sequences from Tseng et al. (2023), and a host of other *Reticulitermes* mitochondrial genome sequences obtained from GenBank, to form the dataset for phylogenetic analysis (Table S2). Each of the 3 loci (16S rRNA, COI, and COII) was aligned independently using MAFFT version 7 with the global pairwise alignment algorithm (G-INS-i method) (Katoh and Standley 2013) and then trimmed to remove all over-hangs. Subsequently, the aligned 16S rRNA, COI, and COII sequences were concatenated using a custom Python script to form a combined dataset comprising 361 bp of 16s, 628 bp of COI, and 680 bp COII. The concatenated sequences were then divided into 7 partitions, 16S rRNA, the 3 codon positions of COI, and the 3 codon positions of COII. The codon positions were confirmed manually using MEGA 11 (Tamura et al. 2021). The best-fit substitution model for each partition was determined using ModelFinder in IQ-TREE (Kalyaanamoorthy et al. 2017). Details of each partition and the selected models are provided in Table S3. Phylogenetic reconstruction was performed using maximum likelihood analyses with IQ-TREE version 2.1.4-beta (Minh et al. 2020). The settings included ultrafast bootstrap (UFBoot) with 10,000 iterations, a maximum correlation coefficient of 0.99, and single-branch tests utilizing the SH-like approximate Likelihood-Ratio Test (SH-aLRT). All other options were set to default. P-distance between sequences was calculated using dist.dna() function in the R package "ape" (Paradis and Schliep 2019).

Short Tandem Repeat Genotyping

Seven microsatellite loci were selected for short tandem repeat (STR) genotyping. These loci were originally developed for *Reticulitermes santonensis* (now a junior synonym of *R. flavipes*) and *R. flavipes* (Vargo 2000, Dronnet et al. 2004) and were later determined to be applicable to *R. hesperus* and related species, providing adequate polymorphism for population-level analyses (Copren 2007). A summary of the general information for each locus is provided in Table S4. Microsatellite genotyping was performed using a 2-step PCR protocol (Blacket et al. 2012). In the initial PCR, the STR region was amplified with locus-specific primers. Fluorescence labeling was incorporated in the second PCR by using 1 of 2 fluorophore-labeled universal primers (Fam or Hex). Thermal cycling conditions for both PCR steps included an initial denaturation at 95 °C for 10 min, followed by 35 cycles at 95 °C for 30 s, annealing at the locus-specific temperature (listed in Table S4) for 30 s, and extension at 72 °C for 30 s, concluding with a final extension at 72 °C for 10 min. The labeled PCR products were analyzed using the fragment analysis service at the Arizona Genetics Core Facility. The resulting raw data were subsequently trimmed, and allele fragment lengths were determined using GeneMarker version 3.0.1 (SoftGenetics, USA).

Genetic Clustering Analysis

To determine whether the *Reticulitermes* clades represented genetically distinct groups, we performed clustering analyses using Principal Coordinates Analysis (PCoA) and the Bayesian model-based approach implemented in STRUCTURE. The sampling sites for genotyped samples are displayed on the map (Fig. 1) and highlighted in red font on the tree (Fig. 3). Detailed information is provided in Table S1. First, genetic clustering patterns were visualized via PCoA based on genetic distance. This analysis was conducted using GenAlEx 6.5 (Peakall and Smouse 2006), an Excel-based tool for population genetic analyses. Subsequently, STRUCTURE version 2.3.4 (Pritchard et al. 2000) was used to evaluate genetic variation and potential gene flow. The number of genetic clusters (K) tested ranged from 1 to 7, with 10 replicates per K value. Each STRUCTURE run included 1,000,000 Markov chain Monte Carlo iterations, discarding the initial 100,000 iterations as burn-in. The optimal K value was determined using Structure Selector (Li and Liu 2018) based on 4 criteria: the ΔK method (Evanno et al. 2005), the LnP(K) method (Pritchard et al. 2000), the median-based MedMedK and MaxMedK methods (Puechmaille 2016). Results from the STRUCTURE analyses were visualized and summarized using the CLUMPAK server (Kopelman et al. 2015). Final graphical representations of population clustering were created with the ggplot2 package in R (Wickham 2016). Additionally, to evaluate how well our predefined groupings based on species and populations are supported by microsatellite data, we conducted a population assignment analysis using GenAlEx 6.5 (Peakall and Smouse 2006). The predefined grouping methods are shown in Fig. 4B beneath the STRUCTURE plot.

Morphological Examination

We initially applied the soldier-caste identification key to identify the specimens we collected in southern California (Banks and Snyder 1920). To evaluate the morphological characteristics, we measured key dimensions of the imago and soldier using high-resolution images captured with a Leica DMS1000 digital microscope (Leica Camera, Wetzlar, Germany) (Fig. 2). The measurements for soldiers included 8 characteristics: pronotum length (PL), pronotum width (PW), head length excluding the mandible (HL), head width at the maximum width of the postmentum (HW), front width of the postmentum (FP), maximum width of the postmentum (MaP), minimum width of the postmentum (MiP), and length of the left mandible (LM) (Fig. 2A and B). Additionally, 8 characteristics were measured for both male and female imago specimens, which included PL, PW, head length to clypeus (HLC), HW, eye length (EL), distance between the eye and ocellus (EO), forewing length (FwL), and hindwing length (HwL) (Fig. 2C to F). All measurements were conducted using high-resolution images digitally captured with a Leica DMS1000 digital microscope and analyzed with Leica LAS X software (version 5.1.1).

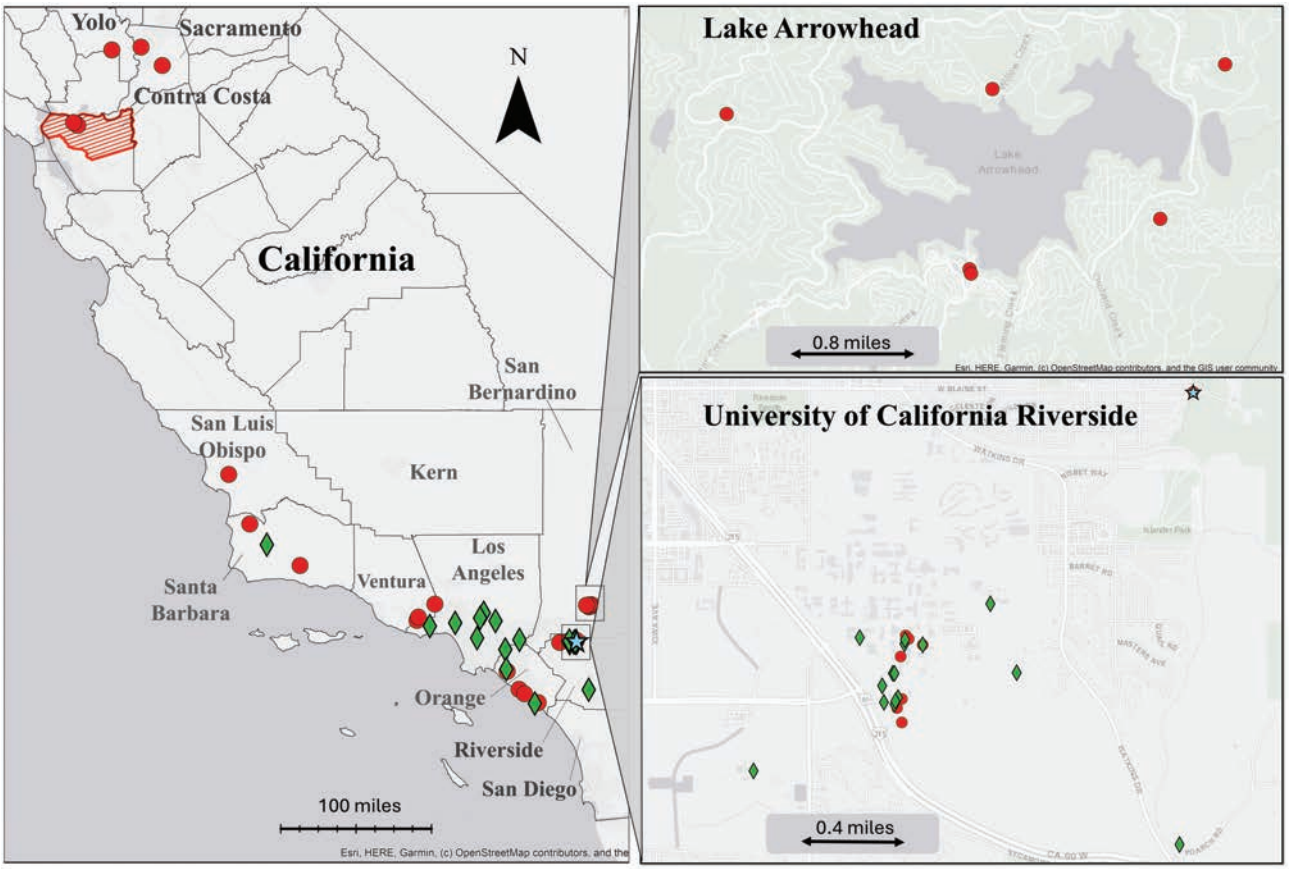

Fig. 1. Map illustrating the sympatric distribution of *Reticulitermes hesperus* and *R. rusti* sp. nov., along with a single *R. tibialis* sample collected in Riverside, CA. The map displays 66 samples used for microsatellite genotyping. The left panel shows the overall distribution of collection sites across the state, while the right panels provide detailed zoom-ins of the Lake Arrowhead and University of California Riverside collection areas. Different markers represent different species: red circles indicate *R. hesperus*, green diamonds represent *R. rusti*, and blue stars mark *R. tibialis*. Contra Costa County is highlighted in red, encompassing one *R. hesperus* sample (Rh08), although GPS coordinates for this site was not recorded.

Colony information and the number of specimens examined are detailed in Table S5 for soldiers and Table S6 for imagoes.

Statistical Analyses

All statistical analyses related to morphological comparisons were conducted using the R statistical programming language (version 4.4.1; R Core Team 2024). For soldier measurements, the *colony* was included as a random effect to account for measurements taken within the same colonies. The data were analyzed using linear mixed models (LMM) with the "lme4" package (Bates et al. 2015) . Posthoc comparisons were made using the "emmeans" package with Tukey adjustment (Lenth 2024). The imagoes of *R. hesperus* and *R. rusti* were compared using the Wilcoxon rank-sum test, implemented via the "wilcox.test" function. All boxplots were generated with the ggplot2 package (Wickham 2016). Additionally, we utilized the dataset comprising all morphological characters to perform multivariate statistical analyses through Permutational Multivariate Analysis of Variance (PERMANOVA), using the "adonis2" function from the "vegan" package (Oksanen et al. 2024). Soldiers and imagoes were analyzed separately. The multivariate results were visualized using principal component analysis (PCA) with the "prcomp" function. Missing values for some individuals were handled using the "imputePCA" function from the "missMDA" package (Josse and Husson 2016). The results were visualized using ggplot2 (Wickham 2016).

Nomenclature

This paper and its nomenclatural act have been registered in Zoobank (www.zoobank.org), the official register of the International Commission on Zoological Nomenclature. The LSID (Life Science Identifier) number of the publication is: urn:lsid:zoobank.org:pub:9DA6D8F7-68DD-4A15-99C8-4F5C6181C2FA. Abbreviations of depository institutions for voucher specimens are as follows: AMNH (American Museum of Natural History, New York, NY, USA), EMEC (Essig Museum of Entomology, University of California, Berkeley, CA, USA), ERM (Entomology Research Museum, University of California, Riverside, CA, USA), UCR (UCR Urban Entomology Laboratory Collection, University of California, Riverside, CA, USA).

Results

Phylogenetic Analysis

The phylogenetic tree reconstructed using concatenated 16S rRNA, COI, and COII sequences clustered samples from the western US into 5 distinct clades (Fig. 3). Clade 5 has previously been identified as *R. hesperus* by Copren et al. (2005), Nelson et al. (2008), and Tseng et al. (2023). Among the 5 Californian clades, the *R. hesperus* clade exhibited the highest divergence from the other 4 in 16S rRNA, COI, and COII (mean *p*-distances: 16S: 3.34% to 3.62%, COI: 7.46% to 9.13%, COII:

7.34% to 8.55%, Table 1). This clade is sister to the eastern US *Reticulitermes* species; however, support for this relationship was weak, indicated by moderate ultrafast bootstrap values (UFBoot: 77%, Fig. 3) and low SH-like approximate Likelihood-Ratio Test values (SH-aLRT: 24.6%, Fig. S1). Clades 1, 2, 3, and 4 formed a monophyletic group. Based on morphology and distribution, we designated Clade 4 as the *R. tibialis* group (see Morphological Examination section). The mean *p*-distances to the other 3 clades were as follows: 16S: 2.35% to 2.97%, COI: 5.67% to 6.01%, and COII: 6.13% to 6.92% (Table 1). Samples in Clade 1 were all collected in southern California. Clade 2 includes samples from Tseng et al. (2023) that were collected in Placerville (El Dorado County), situated in the Sierra Nevada foothills of northern California. Clade 3 consists of samples from various locations in northern California, with the southernmost sample collected in King City, Monterey County (R141). The *p*-distances among these 3 clades were: 16S: 1.35% to 1.77%, COI: 3.51% to 3.87%, and COII: 3.21% to 3.41% (Table 1). In contrast to Tseng et al. (2023), where only 2 lineages were identified in southern California, we collected samples representing 3 independent mtDNA lineages: the remaining *R. hesperus* Clade (Clade 5), the SC-B clade (Clade 1), and an additional species, *R. tibialis* (Clade 4).

Genetic Clustering Analyses

Genetic clustering analyses were performed using microsatellite genotype data to assess whether the 3 clades collected in southern California represent genetically distinct species. Samples were categorized according to the clades identified in the mtDNA phylogenetic tree (Fig. 3). In *R. hesperus* (Clade 5), samples were further divided into northern and southern US populations based on additional genetic cluster analyses.

PCoA showed that the samples grouped into 4 distinct genetic clusters (Fig. 4A). The samples from *R. rusti* (Clade 1; green triangles) and *R. tibialis* (Clade 4; blue circles) each formed independent clusters. In contrast, *R. hesperus* samples (Clade 5; red squares and yellow diamonds) were divided into 2 clusters: one included samples from northern California and Lake Arrowhead (yellow diamonds) and the other comprised samples collected in southern California (red squares).

Due to the limited representation of *R. tibialis*, with only one colony (R66) collected, this sample was excluded from the STRUCTURE analysis to prevent sampling bias that could produce misleading results. The STRUCTURE analysis of the remaining samples identified 3 distinct genetic clusters ($K = 3$): *R. rusti* (green), the northern population of *R. hesperus* (yellow), and the southern population of *R. hesperus* (red) (Fig. 4B). This result corroborates the findings from the PCoA. The optimal number of clusters, $K = 3$, was consistently determined using 4 different methods: the ΔK method (Evanno et al. 2005), the LnP(K) method (Pritchard et al. 2000), and the median-based MedMedK and MaxMedK methods (Puechmaille 2016) (Fig. S2). Despite sample R096 being identified in Lake Arrowhead, no admixed individuals were found. This individual possessed allele "289" at the RS33 locus, which is exclusively found in individuals from *R. rusti* (Clade 1). The genetic assignment analysis

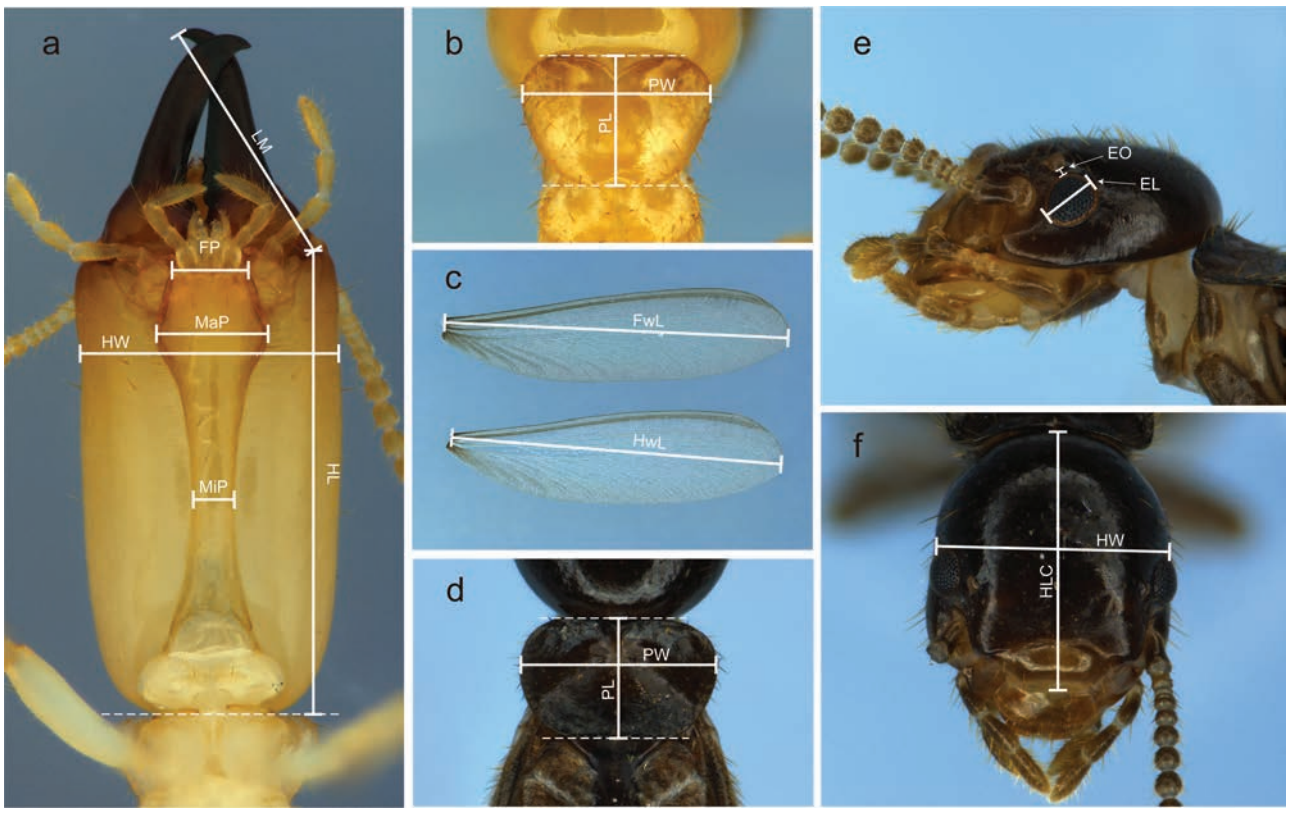

Fig. 2. Morphological measurement characters. For the soldier caste: A) head length excluding mandibles (HL), head width at the maximum width of the postmentum (HW), front width of the postmentum (FP), maximum width of the postmentum (MaP), minimum width of the postmentum (MiP), length of the left mandible (LM); B) pronotum length (PL), pronotum width (PW). For the imago: C) forewing length (FwL), hindwing length (HwL); D) pronotum length (PL), pronotum width (PW); E) eye length (EL), eye to ocellus (EO); F) head length to clypeus (HLC), head width (HW).

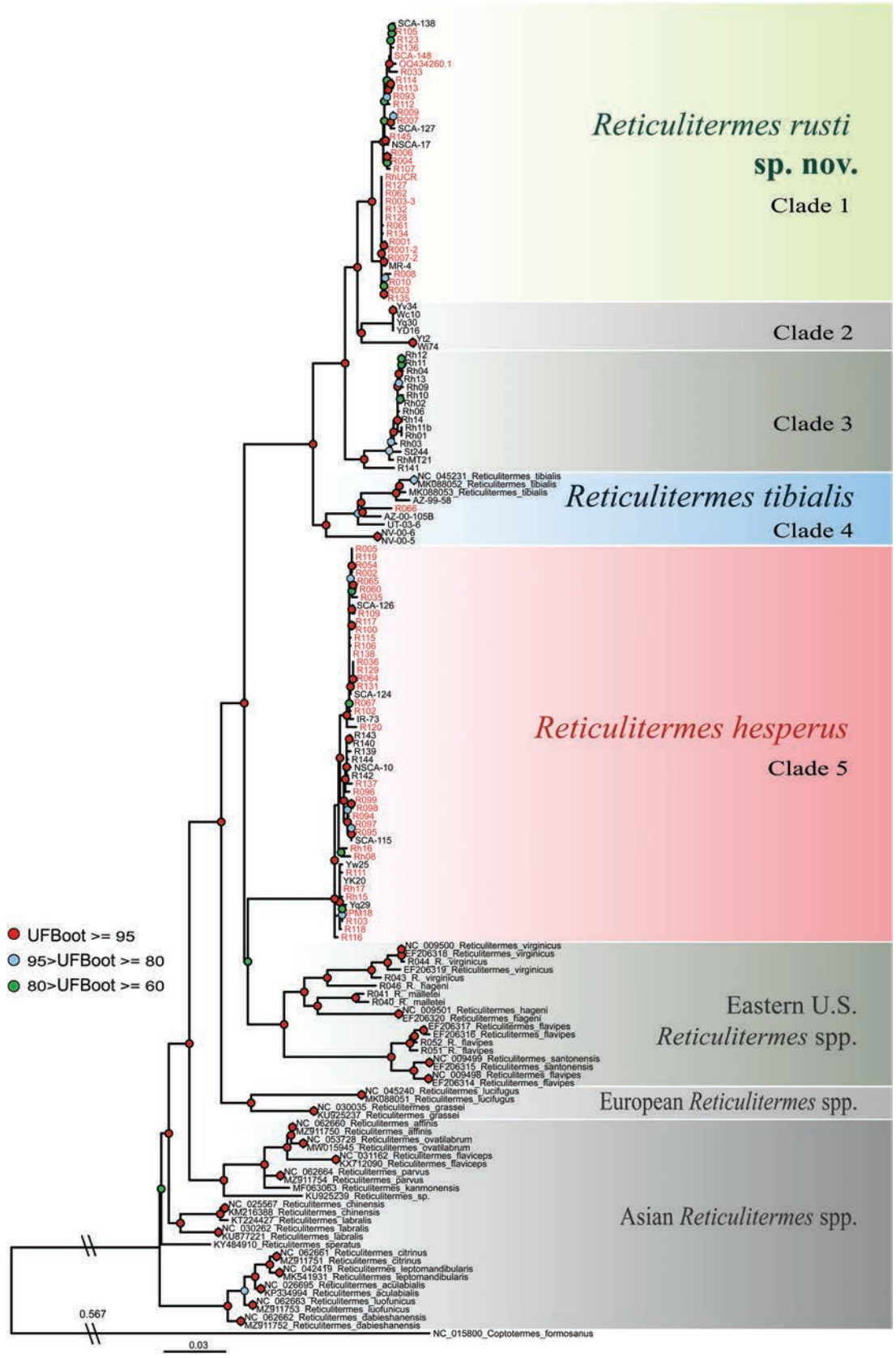

Fig. 3. Phylogenetic tree based on concatenated 16S rRNA (361 bp), COI (628 bp), and COII (680 bp) sequences, illustrating the clustering of *Reticulitermes* species. Clades 1 to 5 represent 5 lineages of *Reticulitermes* in the western US, with 3 clades collected in southern California (*R. rusti* sp. nov. in Clade 1, *R. tibialis* in Clade 4, and *R. hesperus* in Clade 5) highlighted in color. The tree also includes gene sequences from *Reticulitermes* species in the eastern US, Europe, and Asia. Ultrafast bootstrap (UFBoot) is annotated on each node, with values ≥ 95 marked in red, ≥80 marked in blue, and ≥60 marked in green. Values below 60 are not shown. A tree with SH-aLRT is provided in Fig. S2. The branch length to the outgroup is omitted, and the actual genetic distance is directly indicated at the root. Genotyped samples are marked in red font.

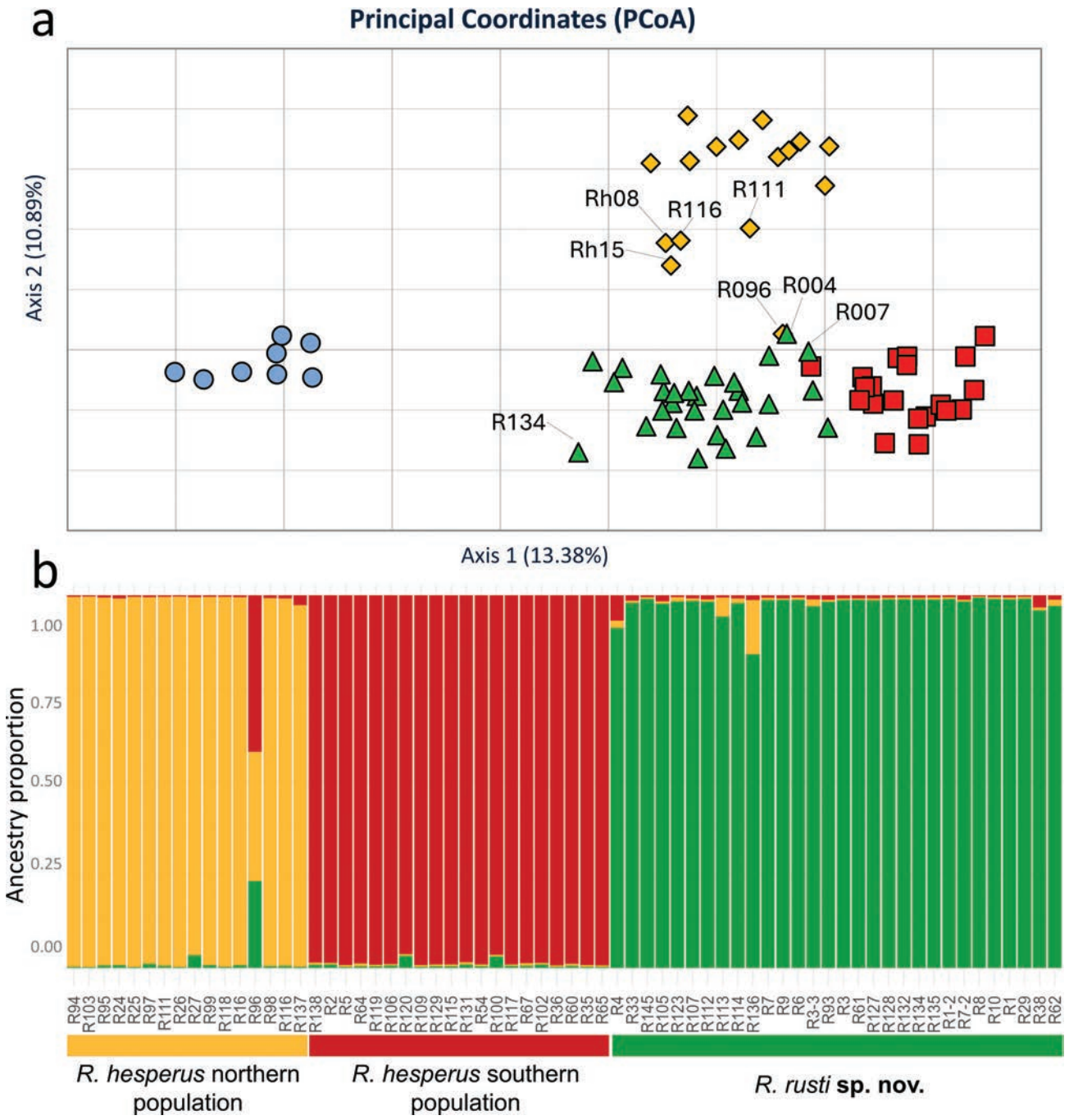

Fig. 4. A) PCoA and B) STRUCTURE analysis of *Reticulitermes* populations. The samples were categorized into 4 predefined groups based on phylogenetic inference: *R. hesperus* northern population includes Clade 5 samples from northern California and Lake Arrowhead, *R. hesperus* southern population includes Clade 5 samples from southern California, *R. rusti* sp. nov. includes samples from Clade 1, and *R. tibialis* corresponds to Clade 4. A) PCoA plot showing the clustering of individuals, with colors representing the predefined grouping of the four populations: *R. hesperus* southern population (red squares), *R. hesperus* northern population (yellow diamonds), *R. rusti* (green triangles), and *R. tibialis* (blue circles). B) STRUCTURE analysis with $K = 3$, displaying the ancestry proportions of individuals. Samples are separated into 3 ancestry groups: *R. hesperus* northern population (yellow), *R. hesperus* southern population (red), and *R. rusti* (green). The color bar at the bottom reflects the predefined grouping method. *R. tibialis* is not included in the STRUCTURE analysis due to the limited sample size ($n = 1$), which could lead to inaccurate clustering.

revealed that our predefined groupings, based on species (*R. hesperus* and *R. rusti*) and populations (*R. hesperus* from northern and southern California), were 98% accurate. The only discrepancy was sample "R096", initially classified as belonging to the northern California population but later assigned to the southern California *R. hesperus* group.

Morphological Examination

After confirming that Clade 1, Clade 4, and Clade 5 represent 3 genetically distinct groups, we identified these clades as separate species by comparing morphological traits and referencing previous descriptions. We first recognized Clade 4 as *R. tibialis* for 2 reasons: (i) according to the soldier-caste identification key (Banks

Table 1. Mean pairwise *p*-distance across different lineages, with values presented for 16S rRNA (top), COI (middle), and COII (bottom) sequences

Mean pairwise *p*-distance between 16S rRNA sequences (%)					
	R. hesperus	***R. tibialis***	***R. rusti***	Clade 2	Clade 3
R. hesperus	0.28 ± 0.25	3.49 ± 0.42	3.45 ± 0.69	3.34 ± 0.31	3.62 ± 0.42
R. tibialis		1.92 ± 0.79	2.35 ± 0.70	2.86 ± 0.53	2.97 ± 0.51
R. rusti			0.83 ± 0.58	1.77 ± 0.65	1.35 ± 0.42
Clade 2				1.09 ± 1.06	2.01 ± 0.26
Clade 3					0.45 ± 0.43
Mean pairwise *p*-distance between COI sequences (%)					
	R. hesperus	***R. tibialis***	***R. rusti***	Clade 2	Clade 3
R. hesperus	1.20 ± 1.36	9.13 ± 0.62	7.50 ± 0.55	7.46 ± 0.96	7.74 ± 0.42
R. tibialis		4.26 ± 1.73	5.81 ± 0.69	6.01 ± 1.10	5.67 ± 0.75
R. rusti			0.93 ± 0.56	3.51 ± 0.40	3.87 ± 0.41
Clade 2				2.29 ± 2.22	4.33 ± 0.44
Clade 3					0.96 ± 0.94
Mean pairwise *p*-distance between COII sequences (%)					
	R. hesperus	***R. tibialis***	***R. rusti***	Clade 2	Clade 3
R. hesperus	0.95 ± 0.52	7.34 ± 0.56	7.98 ± 0.34	8.55 ± 0.25	8.16 ± 0.28
R. tibialis		3.37 ± 1.38	6.13 ± 0.50	6.92 ± 0.61	6.69 ± 0.61
R. rusti			0.89 ± 0.58	3.21 ± 0.35	3.41 ± 0.22
Clade 2				1.85 ± 1.78	3.84 ± 0.66
Clade 3					0.57 ± 0.81

and Snyder 1920), we identified the single sample (R066) in Clade 4 as *R. tibialis* (Fig. 6K to O). (ii) The distribution data aligns with the original description, including sequences from Nevada (NV-00-5 and NV-00-6), Utah (UT-03-6), Arizona (AZ-00-105B and AZ-99-58), and California (R066, Fig. 1). Specimens in Clade 1 and Clade 5 were both initially classified as *R. hesperus*, rendering the group paraphyletic. Measurements of the soldier head capsule indicated that Clade 5 is generally larger, although there is overlap across all measured characters (Table 2, Fig. 5A and Fig. S3). Based on 3 pieces of evidence, we identified Clade 5 as *R. hesperus*: (i) specimens collected from the *R. hesperus* type location, Lake Arrowhead (R95 to R99), fell into Clade 5; (ii) the original distribution descriptions for *R. hesperus* in Banks and Snyder (1920) include northern California, whereas Clade 1 was only found in the southern region; (iii) both holotype and cotype are imagoes originally collected in spring, indicating that this species swarms during the spring season. The cotype was collected at Little Bear Lake (currently known as Lake Arrowhead) (Robinson 1989), San Bernardino Co., California, on 1 June 1917 (Banks and Synder 1920; p. 84). The paratype was collected in the San Gabriel Mountains, Los Angeles Co., California, on 26 March (Banks and Synder 1920, p. 84; Harvard University and Morris 2024). In this study, the 6 *R. hesperus* imagoes we examined (Clade 5) also swarmed in spring, reinforcing the conclusion that Clade 5 represents *R. hesperus*. Consequently, we designated Clade 1 as a new species.

To summarize our measurement data, we conducted a PCA on all measured characters, along with PERMANOVA statistical analysis (Fig. 5). In soldiers, although *R. rusti* and *R. hesperus* exhibited overlapping areas, the PERMANOVA analysis revealed significant differences (Fig. 5A; $F = 30.63499$, $P = 0.001$). In imagoes, despite the morphological distinction being clearer between *R. rusti* and *R. hesperus* (see Description), PERMANOVA did not indicate significant differences (Fig. 5B; $F = 1.849736$, $P = 0.227$).

Taxonomy

Reticulitermes rusti **Chen sp. nov. (Tables 2 and 3, Figs. S3 to S6, Figs. 5 to 8).**

LSID: urn:lsid:zoobank.org:act:F552E898-8B3A-400A-9F4D-94CD47CDC934.

Materials Examined

HOLOTYPE: United States: California: 1 female imago, University of California, Riverside (33°58′08″ N 117°19′37″ W), 02-xi-2023, J.T.C. Chen (AMNH), UCR collection reference: R007.

PARATYPES: United States: California: 1 female imago, University of California, Riverside (33°58′08″ N 117°19′37″ W), 02-xi-2023, J.T.C. Chen (AMNH), UCR collection reference: R007; 1 female imago, University of California, Riverside (33°58′05.1″ N 117°19′34.5″ W), 06-xi-2023, J.T.C. Chen (AMNH), UCR collection reference: R009; 1 soldier, University of California, Riverside (33°58′22.2″ N 117°19′14.9″ W), 16-viii-2023, J.T.C. Chen (EMEC), UCR collection reference: R003; 1 soldier, Los Angeles County (34°12′07.8″ N 118°11′52.4″ W), 2005, W. Studenmund,

Table 2. Morphological measurements of *R. hesperus*, *R. rusti*, and *R. tibialis* soldiers. The table includes the mean, standard deviation (std. dev.), minimum (Min), and maximum (Max) values for various morphological characters: pronotum length (PL), pronotum width (PW), head length excluding mandible (HL), head width at the maximum width of the postmentum (HW), front width of the postmentum (FP), maximum width of the postmentum (MaP), minimum width of the postmentum (MiP), length of the left mandible (LM), and the ratios of MaP/MiP, HL/HW, and HL/LM. The letters next to the means reflect the results of the statistical analysis performed using a linear mixed model. Different letters indicate significant differences based on posthoc comparisons with Tukey's adjustment ($P < 0.05$)

Characters		PL (mm)	PW (mm)	HL (mm)	HW (mm)	FP (mm)	MaP (mm)	MiP (mm)	LM (mm)	MaP/ MiP	HL/ HW	HL/LM
R. hesperus (Colony = 13, *n* = 36)	Mean	0.73 (a)	1.15 (b)	2.63 (b)	1.48 (b)	0.42 (b)	0.64 (b)	0.25 (a)	1.42 (b)	2.59 (b)	1.78 (b)	1.85 (b)
	std. dev.	0.04	0.05	0.19	0.06	0.04	0.03	0.03	0.06	0.23	0.10	0.12
	Min	0.59	1.01	2.06	1.37	0.31	0.58	0.21	1.28	2.10	1.49	1.57
	Max	0.83	1.23	2.98	1.63	0.52	0.72	0.30	1.54	3.05	1.97	2.04
R. rusti (Colony = 12, *n* = 29)	Mean	0.68 (a)	1.03 (a)	2.31 (a)	1.35 (a)	0.36 (a)	0.60 (a)	0.25 (a)	1.25 (a)	2.39 (a)	1.71 (b)	1.85 (b)
	std. dev.	0.05	0.07	0.16	0.08	0.04	0.04	0.04	0.07	0.27	0.05	0.08
	Min	0.60	0.90	1.97	1.21	0.25	0.53	0.19	1.12	1.58	1.62	1.63
	Max	0.77	1.15	2.54	1.53	0.41	0.66	0.38	1.35	2.90	1.81	1.99
R. tibialis (Colony = 1, *n* = 5)	Mean	0.62 (a)	1.09 (ab)	2.02 (a)	1.34 (ab)	0.36 (ab)	0.40 (ab)	0.32 (b)	1.39 (ab)	2.01 (a)	1.51 (a)	1.45 (a)
	std. dev.	0.04	0.05	0.04	0.02	0.04	0.03	0.02	0.04	0.11	0.03	0.03
	Min	0.55	1.05	1.95	1.31	0.25	0.36	0.29	1.35	1.81	1.49	1.41
	Max	0.65	1.19	2.06	1.37	0.41	0.45	0.36	1.45	2.14	1.56	1.49

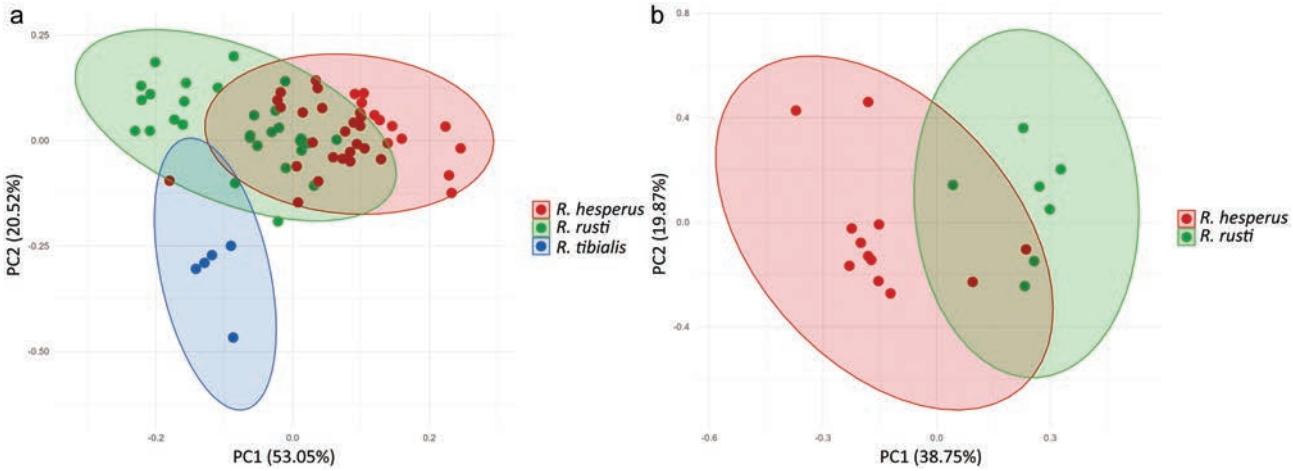

Fig. 5. PCA was performed to examine the morphological variation in *Reticulitermes* soldiers and imagoes. A Permutational Multivariate Analysis of Variance (PERMANOVA) was conducted to assess differences within each group. In soldiers, the multivariate morphological comparison revealed significant differences (A; $F = 30.63499$, $P = 0.001$), whereas in imagoes, no significant differences were detected (B; $F = 1.849736$, $P = 0.227$).

(ERM), UCR collection reference: R105; 1 soldier, University of California, Riverside (33°58′22.2″ N 117°19′14.9″ W), 24-v-2024, C. N. Campbell, (UCR), UCR collection reference: R135; 1 soldier, Los Angeles County (34°05′47″ N 118°42′56″ W), 29-vii-2024, J.T.C. Chen, (UCR), UCR collection reference: R136; 1 soldier, Santa Barbara County (34°44′27.7″ N 120°16′46.4″ W), 1-viii-2024, J.T.C. Chen, (UCR), UCR collection reference: R145.

Other Material Examined

Please see Table S5 for soldier specimens and Table S6 for imago specimens.

Soldier: Color yellowish, similar to *R. hesperus*, paler than *R. tibialis*. Head margins parallel. HL measured at the widest point of postmentum nearly identical to HL measured at the narrowest point. The HL 1.62 to 1.81 times the HW. The pronotum emarginate both in the middle front and the middle rear. LM 1.12 to 1.38 mm. The outer margin of the left mandible is S-shaped, similar to *R. hesperus*, S-shaped but less curved in *R. tibialis*. HL 1.63 to 1.99 times the LM. The widest part of the postmentum is 1.58 to 2.39 times the narrowest part (MiP). *R. rusti* is generally smaller than *R. hesperus*, although size overlaps occur (Fig. 5A, Figs. S3 and S4).

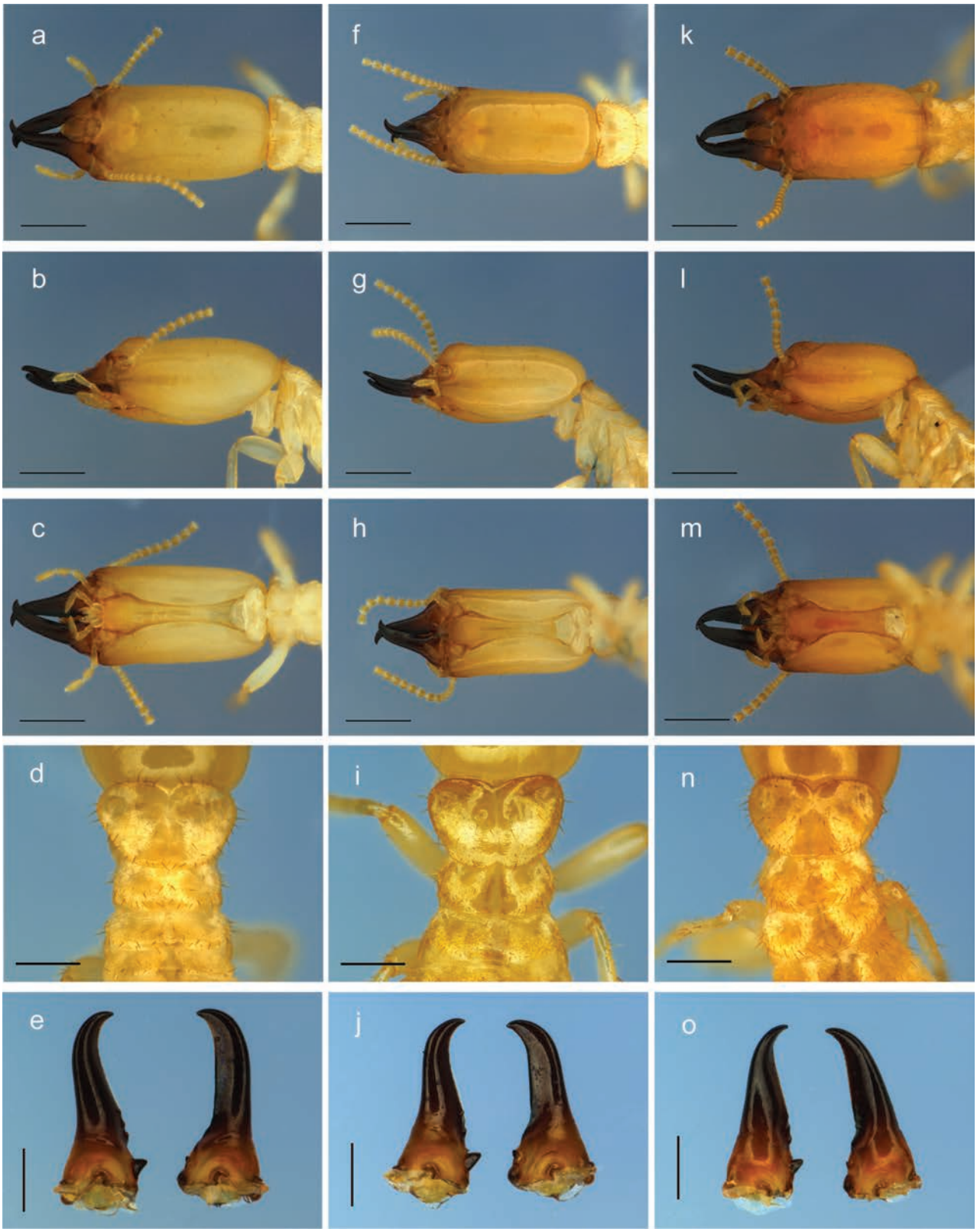

Fig. 6. Morphological features of *Reticulitermes* soldiers. LSID: urn:lsid:zoobank.org:act:F552E898-8B3A-400A-9F4D-94CD47CDC934. Each row represents a different species: *R. hesperus* (A to E), *R. rusti* sp. nov. (F to J), and *R. tibialis* (K to O). Each column displays different views of the species: dorsal view of the head capsule (A, F, K), lateral view of the head capsule (B, G, L), ventral view of the head capsule (C, H, M), dorsal view of the pronotum (D, I, N), and dorsal view of the mandibles (E, J, O). The scale bar is 1 mm for images A to C, F to H, and K to M, and 500 μm for images D, E, I, J, N, and O.

Table 3. Morphological measurements of *R. hesperus* and *R. rusti* imagoes (female and male). The table includes mean, standard deviation (std. dev.), minimum (Min), and maximum (Max) values for various morphological characters: pronotum length (PL), pronotum width (PW), head length to clypeus (HLC), head width (HW), eye length (EL), eye to ocellus (EO), forewing length (FwL), and hindwing length (HwL). Statistical analysis was performed using the Wilcoxon signed rank test. An asterisk (*) indicates significant differences ($P < 0.05$).

Characters		PL (mm)	PW (mm)	HLC (mm)	HW (mm)	EL (mm)	EO (μm)	FwL* (mm)	HwL* (mm)
R. hesperus Imago ♀ (n = 6, Total = 6)	Mean	0.67	1.07	1.30	1.21	0.29	34.26	9.01	8.85
	std. dev.	0.02	0.04	0.06	0.03	0.01	2.95	0.55	0.49
	Min	0.66	1.05	1.25	1.15	0.27	30.15	8.25	8.11
	Max	0.69	1.13	1.42	1.23	0.30	38.13	9.76	9.38
R. hesperus Imago ♂ (n = 6, Total = 6)	Mean	0.65	1.05	1.33	1.21	0.27	39.71	8.74	8.55
	std. dev.	0.03	0.03	0.06	0.04	0.02	10.97	0.37	0.37
	Min	0.64	1.02	1.26	1.19	0.26	30.02	8.04	7.89
	Max	0.68	1.09	1.42	1.28	0.29	59.93	9.12	9.01
R. rusti Imago ♀ (n = 4, Total = 4)	Mean	0.65	1.04	1.26	1.21	0.26	34.96	10.90	10.47
	std. dev.	0.02	0.02	0.02	0.03	0.02	4.54	0.25	0.36
	Min	0.62	1.02	1.23	1.17	0.24	28.76	10.52	10.03
	Max	0.68	1.06	1.29	1.25	0.28	40.75	11.20	11.02
R. rusti Imago ♂ (n = 3, Total = 3)	Mean	0.60	1.01	1.26	1.18	0.27	38.11	10.31	9.93
	std. dev.	0.01	0.02	0.01	0.03	0.00	7.28	0.04	0.18
	Min	0.59	0.99	1.25	1.14	0.27	29.55	10.26	9.79
	Max	0.62	1.04	1.27	1.21	0.28	47.34	10.35	10.18

Imago: Sclerotized area deep black. HLC slightly longer than the HW; eyes about circular, diameter 0.24 to 0.28 mm. Ocelli very close to eyes (EO: 28.76 to 47.34 μm), EO shorter than eye-to-antennal socket distance. Antennae color brownish, darker than *R. hesperus*. Tibiae dark brown to black, paling only at the end of the tibiae. Tarsi pale yellowish. Paraprocts brownish. Wings transparent to pale brownish, more transparent than *R. hesperus*. FwL 10.52 to 11.20 mm. HwL 9.79 to 11.02 mm. The body length, excluding wings, is equal to or greater than the length from the abdomen end to the wing tips (Fig. 8).

Diagnosis

Of the southern California *Reticulitermes*, *R. rusti* is genetically closest to *R. tibialis*, but the soldier can be distinguished by a larger HL to LM ratio: 1.63 to 1.99 in *R. rusti* versus 1.41 to 1.49 in *R. tibialis*. The *R. rusti* soldier is morphologically very similar but slightly smaller than *R. hesperus* (Table 2, Figs 6 and 8). Soldier identification between the 2 species should be confirmed through COI or COII sequence on GenBank.

The imagoes of *R. rusti* can be distinguished from *R. hesperus* by dark brownish tibiae and longer wing length. For *R. rusti*, FwL: 10.26 to 11.20 mm, HwL: 9.79 to 11.02 mm; for *R. hesperus*, FwL: 8.04 to 9.76 mm, HwL: 7.89 to 9.38 mm (Table 3. Figs. 7 and 8). COI and COII sequences for voucher specimens are available in GenBank (Holotype: R007, COI: PV121365, COII: PV133894; Paratypes: R003, COI: PV121360, COII: PV133872; R009, COI: PV121368, COII: PV133897; R105, COI: PV121397, COII: PV133835; R135, COI: PV121417, COII: PV133856; R136, COI: PV121418, COII: PV133864; R145, COI: PV121426, COII: PV133869).

Ecology and Distribution

This species is commonly found in southern California, with its southernmost distribution possibly extending into Baja California. The northernmost sample was collected in Santa Barbara. Its entire distribution range overlaps with that of *R. hesperus*.

Remarks

Unlike *R. hesperus*, which swarms in the spring, swarms of *R. rusti* occur from late fall to winter (November through January) after the first fall rain. In addition, *R. rusti* possesses the CHC phenotypes SC-B and SC-B′. For further details on its CHC profile, see Nelson et al. (2008).

Etymology

We named this species '*rusti*' in honor of Professor Emeritus Michael K. Rust (University of California, Riverside), who has contributed significantly to our knowledge of the biology and management of subterranean termites in southern California for the last 50 yr.

Discussion

This study employed an integrative taxonomic approach (Padial et al. 2010) that incorporated phylogenetic evidence, the genotypic cluster concept (Mallet 1995), morphological comparisons, and previous chemotaxonomic data based on CHC analyses. Together, these complementary lines of evidence demonstrate the presence of a new subterranean termite species in the genus *Reticulitermes* in southern California. Population clustering analyses distinguish *R. rusti* from *R. hesperus* and *R. tibialis*. Additionally, mtDNA phylogenies reconstructed from 16S, COI, and COII genes indicate that *R. rusti* is genetically closer to *R. tibialis* than to *R. hesperus*. Combined with morphological measurements, flight phenology (Table S6), and CHC phenotype data presented in Nelson et al. (2008) and Tseng et al. (2023), we confirm that the CHC phenotype SC-B and SC-B′ (Clade 1) is a distinct species, separate from *R. hesperus*.

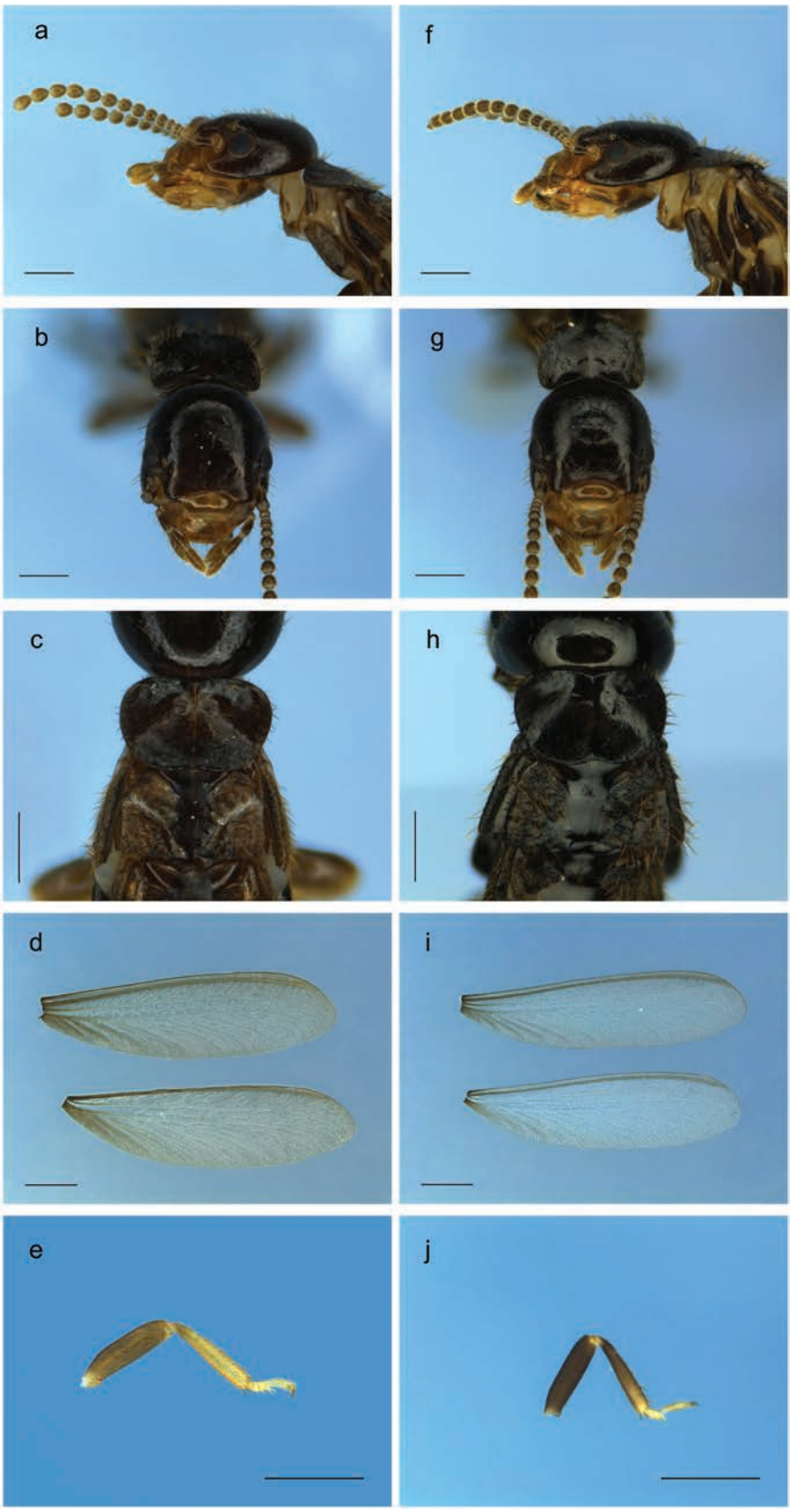

Fig. 7. Morphological features of *Reticulitermes* imagoes. LSID: urn:lsid:zoobank.org:act:F552E898-8B3A-400A-9F4D-94CD47CDC934. Each column represents a different species: *R. hesperus* (A to E) and *R. rusti* sp. nov. (F to J). Each row displays different views of the species: lateral of the head (A, F), dorsal view of the head (B, G), dorsal view of the pronotum (C, H), right wings (D, I), and right middle legs (E, J). For images A to C, E to G, and J, the scale bar represents 500 μm. For images D and I, it represents 2 mm.

Our phylogenetic analysis reveals that the undescribed *Reticulitermes* (Clades 1, 2, and 3) form a monophyletic group, which is sister to *R. tibialis*. In this study, we describe the new species, *R. rusti*, corresponding to Clade 1, while Clades 2 and 3 remain undescribed. The discovery of *R. rusti* and its related clades was initially inferred through CHC analyses (Haverty and Nelson 1997, Copren et al. 2005, Nelson et al. 2008). *R. rusti* aligns with the SC-B and SC-B′ phenotypes, whereas its sister group, Clade 2, corresponds to the CA-B and CA-C phenotypes. Clade 3 is associated with the CA-D phenotype, which is sister to the Clade 2 + *R. rusti* group.

The mean *p*-distance between *R. rusti*, Clade 2, and Clade 3 (16S: 1.35% to 1.77%; COI: 3.51% to 3.87%; COII: 3.21% to 3.41%;) (Table 1) suggest some ambiguity regarding species boundaries, leaving the exact number of species subject to further debate. A genetic distance of approximately 3% in the COI sequence is often used as a threshold for species delimitation in insects and can distinguish up to 98% of lepidopteran species (Hebert et al. 2003). Considering these points, we chose not to assign Clades 2 (CA-B and CA-C) and 3 (CA-D) to *R. rusti* for the following reasons: (i) *Geographic distribution*: the clades exhibit distinct geographic ranges. In Clade 2, CA-B has been found only in El Dorado County, while CA-C has been found in El Dorado, Nevada, Sacramento, and San Joaquin counties in California (Tseng et al. 2023). Clade 3 (CA-D), in contrast, is primarily found in more coastal regions in northern California and is sympatric with *R. hesperus* (Haverty and Nelson 1997, Haverty et al. 2003, Copren et al. 2005, Tseng et al. 2023), (ii) *Distinct CHC profiles*: each clade possesses unique CHC profiles, as detailed by Haverty and Nelson (1997), Copren et al. (2005), and Nelson et al. (2008), (iii) *Statistical evidence*: a multispecies coalescent approach (BPP) employed by Tseng et al. (2023) supports the recognition of 4 independent species within these groups.

Our next step is to examine species boundaries through population-level approaches to strengthen these conclusions. This approach includes applying integrative taxonomy (Padial et al. 2010), accounting for gene flow that may confound phylogenetic inference (Leaché et al. 2014) and conducting integrative species delimitation methods (Singhal et al. 2018) to distinguish valid species lineages from mere population-level variation.

Our morphological measurements successfully distinguished *R. rusti* from both *R. tibialis* in the soldier caste and *R. hesperus* in the imago caste. In the soldier caste, *R. tibialis*, compared with the other 2 species, displays more apparent morphological differences (Figs. 6 and 8). Soldiers have dull brownish head capsules with slightly curved sides, making the head broadest at the point corresponding to the MiP. The outer margin of the left mandible is less curved than that of the other 2 species. In contrast, *R. hesperus* and *R. rusti* both have pale yellowish to yellowish colored head capsules. The sides of the head capsule are parallel, with an approximately equal head length to head width (HL/HW) ratio. The outer margin of the left mandible is S-shaped. Morphometric measurements show that *R. rusti* is relatively similar to but slightly smaller than *R. hesperus*. Due to the overlap in characters, it is not possible to propose diagnostic morphological characters for the soldier caste to distinguish *R. rusti* (Table 2, Figs. 5A and 6). However, in the imago, *R. hesperus* does differ from *R. rusti*. The sclerotized regions of *R. rusti* appear deep black, likely due to heavier sclerotization. The most significant difference is in the tibiae: *R. hesperus* exhibits pale yellowish tibiae, whereas *R. rusti* has dark brown to black tibiae. Additionally, *R. rusti* possesses longer and more transparent wings than *R. hesperus*

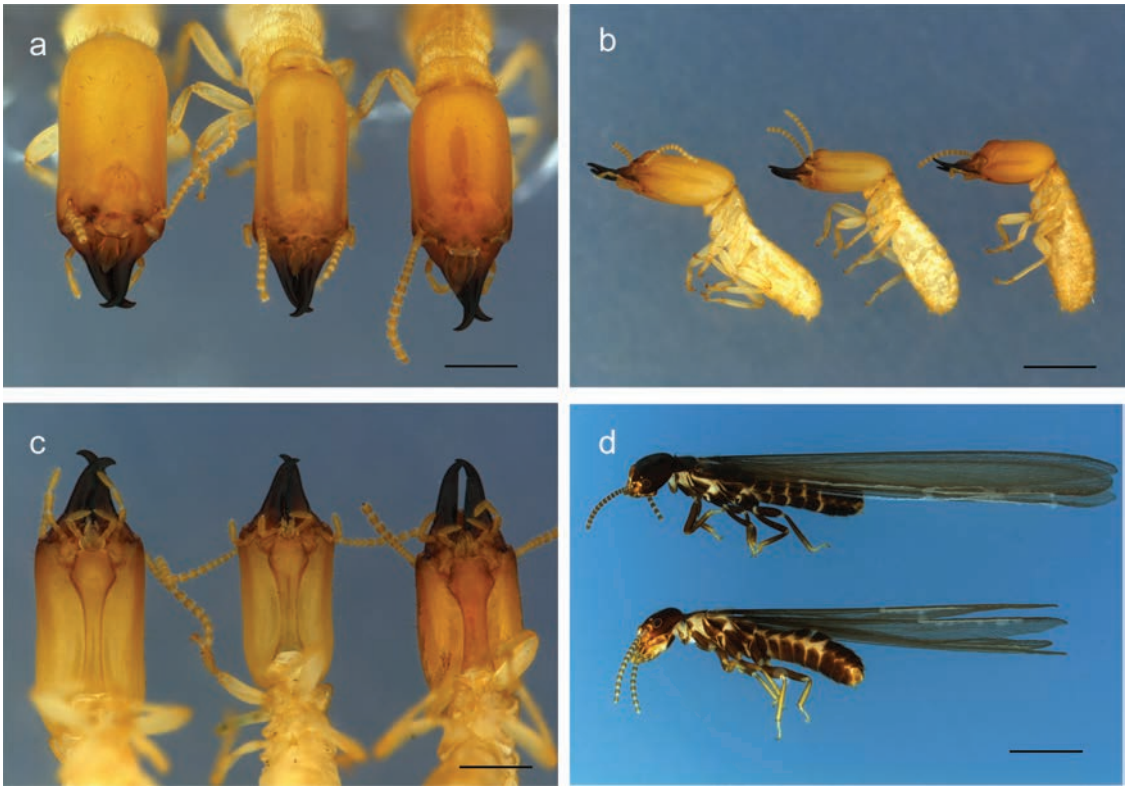

Fig. 8. Morphological comparison of *Reticulitermes hesperus*, *R. rusti* sp. nov., and *R. tibialis*. LSID: urn:lsid:zoobank.org:act:F552E898-8B3A-400A-9F4D-94CD47CDC934. (A to C) Comparison of soldier castes in dorsal (A), lateral (B), and ventral (C) views. From left to right: *R. hesperus*, *R. rusti*, and *R. tibialis*. D) Comparison of the imago (male): top, *R. rusti*; bottom, *R. hesperus*. The scale bar represents 1 mm for images (A) and (C), and 2 mm for images (B) and (D).

(Table 3, Fig 7). In conclusion, *R. rusti* is a new species that could be readily differentiated from *R. hesperus* using the imago stage.

Solely relying on morphological characters to identify species remains challenging because of the difficulty in collecting a sufficient number of alates and soldiers. Therefore, we also recommend using the mtDNA region COI and COII for reliable species identification. We also reclassified historical sequences deposited in GenBank from 5 publications as *R. rusti* in Table S7 (Copren et al. 2005, Su et al. 2006, Tripodi et al. 2006, Wang et al. 2022, Tseng et al. 2023). In the Barcode of Life Data System (BOLD), *R. rusti* is within the Barcode Index Number: 'BOLD:ACP7685' (Ratnasingham and Hebert 2013; https://v3.boldsystems.org/index.php/Public_BarcodeCluster?clusteruri=BOLD:ACP7685).

The fact that these nonsister groups (*R. rusti* and *R. hesperus*) share similar morphology in the soldier caste may be caused by various factors. One possibility is adaptive convergence (Losos 2011), which means the independent evolution of similar features in different lineages. Convergent adaptation can be triggered by environmental pressure (Greenway et al. 2024) or predation pressure (Lee and Coop 2019). Another possible reason causing similar morphology is hybridization-induced gene introgression (Grant et al. 2004, Rosser et al. 2024). Indeed, hybridization among *Reticulitermes* species is not uncommon under laboratory conditions (Pickens 1932, Wu et al. 2019) and can facilitate the exchange of alleles between species. In this study, the result of clustering analysis identified a single individual (R096) with an admixed genetic background. Notably, among the 6 samples collected from type location Lake Arrowhead (R94 to R99), no species other than *R. hesperus* were detected; one individual, however, carried a single allele—'289' at the RS33 locus—that is shared with *R. rusti*. The primary criteria for determining whether 2 species with different swarming seasons can hybridize are the presence of any overlap in their geographical distribution and swarming periods. We observe that the spring swarmers (*R. hesperus*) swarm later in the season in mountain ranges due to the shorter period of suitable weather for swarming. However, we have not collected any *R. rusti* colonies in Lake Arrowhead. Therefore, it remains unknown whether the two species' geographical distributions and swarming seasons overlap in mountain ranges. Since only one locus and one individual exhibit signs of hybridization, more comprehensive genetic data are needed to determine whether genuine hybridization really occurred.

Reticulitermes hesperus has long been recognized as California's most common subterranean termite pest species. Its status as a pest has prompted numerous studies on control strategies of this species, including liquid termiticides (Lewis et al. 1996, Rust and Saran 2006, 2008, Saran and Rust 2007), and baits (Lewis and Power 2006, Eger et al. 2012, Hamm et al. 2013). However, few studies have ever considered the presence of undescribed species (Getty et al. 2007), making it difficult to ascertain whether those studies had evaluated *R. hesperus*, *R. rusti*, or other undescribed taxa. Past studies have reported that it was challenging to bait *R. hesperus* in southern California due to low foraging activity and poor bait station foraging fidelity (Haagsma and Rust 2005). On the contrary, unlike in southern California, baiting *R. hesperus* in northern California did not experience any of those challenges (Getty et al. 2007, Haverty et al. 2010, Sutherland et al. 2022). Could the anomaly in bait responses observed between northern and southern California be attributed to the presence of a different species (*R. rusti*) at the latter location?

This is why accurate species identification is crucial in urban pest management, as different species may exhibit distinct behaviors and biological traits that could influence management strategies (Hapukotuwa and Grace 2012, 2014, Su and Lee 2023). Future research should focus on investigating and comparing the biology and pest status of *R. rusti* and *R. hesperus*. With this knowledge, species-specific pest management strategies can be developed to accurately predict and implement effective measures to mitigate the damage caused by *Reticulitermes* infestations.

Supplementary material

Supplementary material is available at *Annals of the Entomological Society of America* online.

Acknowledgments

We thank Jim Chase (Marietta, GA) and Brian T. Forschler (University of Georgia, Athens) for providing specimens of the eastern US *Reticulitermes* species. We also thank Greg Kund, Emily Ta, Rattanan Chungsawat, Jun-Yin Lum, Xin-Wei Fang, Allen Zhao, and Hoeun Park (UC Riverside) for assistance during field collections. We are grateful to Michael Rust (UC Riverside) and Gillian Gile (Arizona State University) for helpful discussions on *Reticulitermes* in California and Arizona. Additionally, we thank Alan Brelsford and Christiane Weirauch (UC Riverside) for their advice on population genetics, and systematics, respectively. This study was supported by the UC Riverside Urban Entomology Endowed Chair Research Fund. The findings and conclusions in this publication are those of the authors and do not represent any official USDA or US Government determination or policy.

Author contributions

Joanne Tzu-Chia Chen (Conceptualization [equal], Data curation [lead], Formal analysis [lead], Investigation [lead], Methodology [lead], Resources [equal], Validation [lead], Visualization [lead], Writing—original draft [lead], Writing—review & editing [lead]), Lori Nelson (Conceptualization [supporting], Data curation [equal], Resources [equal], Writing—review & editing [equal]), Paul Rugman-Jones (Resources [equal], Writing—review & editing [supporting]), Shu-Ping Tseng (Conceptualization [supporting], Formal analysis [supporting], Writing—review & editing [equal]), Andrew Sutherland (Resources [supporting], Writing—review & editing [supporting]), Dong-Hwan Choe (Supervision [supporting], Writing—review & editing [supporting]), Michael Haverty (Conceptualization [supporting], Resources [equal], Writing—review & editing [equal]), and Chow-Yang Lee (Conceptualization [equal], Funding acquisition [lead], Project administration [lead], Supervision [lead], Writing—original draft [equal], Writing—review & editing [equal])

Conflicts of interest. None declared.

References

Abbott R, Albach D, Ansell S, et al. 2013. Hybridization and speciation. J. Evol. Biol. 26:229–246. https://doi.org/10.1111/j.1420-9101.2012.02599.x

Adams M, Raadik TA, Burridge CP, et al. 2014. Global biodiversity assessment and hyper-cryptic species complexes: more than one species of elephant in the room? Syst. Biol. 63:518–533. https://doi.org/10.1093/sysbio/syu017

Austin J, Szalanski AL, Scheffrahn R, et al. 2005. Genetic variation of *Reticulitermes flavipes* (Isoptera: Rhinotermitidae) in North America applying the mitochondrial rRNA 16S gene. Ann. Entomol. Soc. Am. 98:980–988. https://doi.org/10.1603/0013-8746(2005)098[0980:GVORFI]2.0.CO;2

Banks N, Snyder TE. 1920. A revision of the Nearctic termites. U.S. Nat. Museum Bull. 108:1–228. https://doi.org/10.5479/si.03629236.108.i

Bates D, Mächler M, Bolker B, et al. 2015. Fitting linear mixed-effects models using lme4. J. Stat. Soft. 67:1–48. https://doi.org/10.18637/jss.v067.i01

Blacket MJ, Robin C, Good RT, et al. 2012. Universal primers for fluorescent labelling of PCR fragments--an efficient and cost-effective approach to genotyping by fluorescence. Mol. Ecol. Resour. 12:456–463. https://doi.org/10.1111/j.1755-0998.2011.03104.x

Copren KA. 2007. Characterization of microsatellite loci in the western subterranean termite, *Reticulitermes hesperus*, and cross-amplification in closely related cryptic species. J. Insect Sci. 7:17. https://doi.org/10.1673/031.007.1701

Copren KA, Nelson LJ, Vargo EL, et al. 2005. Phylogenetic analyses of mtDNA sequences corroborate taxonomic designations based on cuticular hydrocarbons in subterranean termites. Mol. Phylogenet. Evol. 35:689–700. https://doi.org/10.1016/j.ympev.2005.03.002

Delphia CM, Copren KA, Haverty MI. 2003. Agonistic behavior between individual worker termites from three cuticular hydrocarbon phenotypes of *Reticulitermes* (Isoptera: Rhinotermitidae) from northern California. Ann. Entomol. Soc. Am. 96:585–593. https://doi.org/10.1603/0013-8746(2003)096[0585:abbiwt]2.0.co;2

Després L. 2019. One, two or more species? Mitonuclear discordance and species delimitation. Mol. Ecol. 28:3845–3847. https://doi.org/10.1111/mec.15211

Dronnet S, Bagnères A-G, Juba TR, et al. 2004. Polymorphic microsatellite loci in the European subterranean termite, *Reticulitermes santonensis* Feytaud: PRIMER NOTE. Mol. Ecol. Notes 4:127–129. https://doi.org/10.1111/j.1471-8286.2004.00600.x

Eger JE Jr, Lees MD, Neese PA, et al. 2012. Elimination of subterranean termite (Isoptera: Rhinotermitidae) colonies using a refined cellulose bait matrix containing noviflumuron when monitored and replenished quarterly. J. Econ. Entomol. 105:533–539. https://doi.org/10.1603/ec11027

Evanno G, Regnaut S, Goudet J. 2005. Detecting the number of clusters of individuals using the software STRUCTURE: a simulation study. Mol. Ecol. 14:2611–2620. https://doi.org/10.1111/j.1365-294X.2005.02553.x

Folmer O, Black MB, Hoeh W, et al. 1994. DNA primers for amplification of mitochondrial cytochrome c oxidase subunit I from diverse metazoan invertebrates. Mol. Mar. Biol. Biotechnol. 3:294–299. https://www.mbari.org/wp-content/uploads/2016/01/Folmer_94MMBB.pdf

Getty GM, Solek CW, Sbragia RJ, et al. 2007. Large-scale suppression of a subterranean termite community using the Sentricon® Termite Colony Elimination System: a case study in Chatsworth, California, USA. Sociobiology 50:1041–1050.

Gleason RW, Koehler PG. 1980. Termites of the eastern and southeastern United States: pictorial keys to soldiers and winged reproductives. *Bulletin 192*. Institute of Food and Agricultural Sciences (IFAS), University of Florida.

Grant PR, Grant BR, Markert JA, et al. 2004. Convergent evolution of Darwin's finches caused by introgressive hybridization and selection. Evolution 58:1588–1599. https://doi.org/10.1111/j.0014-3820.2004.tb01738.x

Greenway R, De-Kayne R, Brown AP, et al. 2024. Integrative analyses of convergent adaptation in sympatric extremophile fishes. Curr. Biol. 34:4968–4982.e7. https://doi.org/10.1016/j.cub.2024.09.027

Haagsma KA, Rust MK. 2005. Effect of hexaflumuron on mortality of the Western subterranean termite (Isoptera: Rhinotermitidae) during and following exposure and movement of hexaflumuron in termite groups. Pest Manag. Sci. 61:517–531. https://doi.org/10.1002/ps.1003

Hamm RL, DeMark JJ, Chin-Heady E, et al. 2013. Consumption of a durable termite bait matrix by subterranean termites (Isoptera: Rhinotermitidae) and resulting insecticidal activity. Pest Manag. Sci. 69:507–511. https://doi.org/10.1002/ps.3401

Hapukotuwa NK, Grace JK. 2012. *Coptotermes formosanus* and *Coptotermes gestroi* (Blattodea: Rhinotermitidae) exhibit quantitatively different tunneling patterns. Psyche 2012:1–7. https://doi.org/10.1155/2012/675356

Hapukotuwa N, Grace JK. 2014. Comparison of *Coptotermes formosanus* and *Coptotermes gestroi* (Blattodea: Rhinotermitidae) field sites and seasonal foraging activity in Hawaii. Sociobiology 59:203–212. https://doi.org/10.13102/SOCIOBIOLOGY.V59I1.677

Harvard University M, Morris PJ. 2024. Museum of Comparative Zoology, Harvard University. Version 162.451. Museum of Comparative Zoology, Harvard University. Occurrence dataset https://doi.org/10.15468/p5rupv accessed via GBIF.org on 2024-12-31. https://www.gbif.org/occurrence/1978872448

Haverty MI, Nelson LJ. 1997. Cuticular hydrocarbons of *Reticulitermes* (Isoptera: Rhinotermitidae) from northern California indicate undescribed species. Comp. Biochem. Physiol. B: Biochem. Mol. Biol. 118:869–880. https://doi.org/10.1016/s0305-0491(97)00237-x

Haverty MI, Nelson LJ. 2007. *Reticulitermes* (Isoptera: Rhinotermitidae) in Arizona: multiple cuticular hydrocarbon phenotypes indicate additional taxa. Ann. Entomol. Soc. Am. 100:206–221. https://doi.org/10.1603/0013-8746(2007)100[206:ririam]2.0.co;2

Haverty MI, Copren KA, Getty GM, et al. 1999. Agonistic behavior and cuticular hydrocarbon phenotypes of colonies of *Reticulitermes* (Isoptera: Rhinotermitidae) from northern California. Ann. Entomol. Soc. Am. 92:269–277. https://doi.org/10.1093/aesa/92.2.269

Haverty MI, Getty GM, Nelson LJ, et al. 2003. Flight phenology of sympatric populations of *Reticulitermes* (Isoptera: Rhinotermitidae) in northern California: disparate flight intervals indicate reproductive isolation among cuticular hydrocarbon phenotypes. Ann. Entomol. Soc. Am. 96:828–833. https://doi.org/10.1603/0013-8746(2003)096[0828:fpospo]2.0.co;2

Haverty MI, Tabuchi RL, Vargo EL, et al. 2010. Response of *Reticulitermes hesperus* (Isoptera: Rhinotermitidae) colonies to baiting with lufenuron in northern California. J. Econ. Entomol. 103:770–780. https://doi.org/10.1603/ec09088

Hebert PDN, Cywinska A, Ball SL, et al. 2003. Biological identifications through DNA barcodes. Proc. Biol. Sci. 270:313–321. https://doi.org/10.1098/rspb.2002.2218

Jenkins T, Haverty M, Basten C, et al. 2000. Correlation of mitochondrial haplotypes with cuticular hydrocarbon phenotypes of sympatric *Reticulitermes* species from the southeastern United States. J. Chem. Ecol. 26:1525–1542. https://doi.org/10.1023/A:1005548111591

Josse J, Husson F. 2016. MissMDA: a package for handling missing values in multivariate data analysis. J. Stat. Softw. 70:1–31. https://doi.org/10.18637/jss.v070.i01

Kalyaanamoorthy S, Minh BQ, Wong TKF, et al. 2017. ModelFinder: fast model selection for accurate phylogenetic estimates. Nat. Methods 14:587–589. https://doi.org/10.1038/nmeth.4285

Kambhampati S, Smith PT. 1995. PCR primers for the amplification of four insect mitochondrial gene fragments. Insect. Mol. Biol. 4:233–236. https://doi.org/10.1111/j.1365-2583.1995.tb00028.x

Katoh K, Standley DM. 2013. MAFFT multiple sequence alignment software version 7: improvements in performance and usability. Mol. Biol. Evol. 30:772–780. https://doi.org/10.1093/molbev/mst010

Kopelman NM, Mayzel J, Jakobsson M, et al. 2015. Clumpak: a program for identifying clustering modes and packaging population structure inferences across K. Mol. Ecol. Resour. 15:1179–1191. https://doi.org/10.1111/1755-0998.12387

Leaché AD, Harris RB, Rannala B, et al. 2014. The influence of gene flow on species tree estimation: a simulation study. Syst. Biol. 63:17–30. https://doi.org/10.1093/sysbio/syt049

Lee KM, Coop G. 2019. Population genomics perspectives on convergent adaptation. Philos. Trans. R. Soc. Lond. B Biol. Sci. 374:20180236. https://doi.org/10.1098/rstb.2018.0236

Lenth RV. 2024. emmeans: estimated marginal means, aka least-squares means. https://CRAN.R-project.org/package=emmeans

Lewis V, Power A. 2006. Evaluation of bait-toxicant transfer among conspecific laboratory populations of *Reticulitermes* spp. from California (Isoptera: Rhinotermitidae). Sociobiology 48:375–383.

Lewis VR, Haverty MI, Carver DS, et al. 1996. Field comparison of sand or insecticide barriers for control of *Reticulitermes* spp. (Isoptera: Rhinotermitidae) infestations in homes in northern California. Sociobiology 23:327–335.

Li Y-L, Liu J-X, Liu J-X. 2018. StructureSelector: a web-based software to select and visualize the optimal number of clusters using multiple methods. Mol. Ecol. Resour. 18:176–177. https://doi.org/10.1111/1755-0998.12719

Light SF, Pickens AL. 1934. American subterranean termites, their classification and distribution. In: Kofoid CA, Light SF, Horner AC, Randall M, et

al. editors. Termites and termite control, 2nd ed. Revised. University of California Press. p. 150–156

Losos JB. 2011. Convergence, adaptation, and constraint. Evolution 65:1827–1840. https://doi.org/10.1111/j.1558-5646.2011.01289.x

Mallet J. 1995. A species definition for the modern synthesis. Trends Ecol. Evol. 10:294–299. https://doi.org/10.1016/0169-5347(95)90031-4

Minh BQ, Schmidt HA, Chernomor O, et al. 2020. IQ-TREE 2: new models and efficient methods for phylogenetic inference in the genomic era. Mol. Biol. Evol. 37:1530–1534. https://doi.org/10.1093/molbev/msaa015

Nelson LJ, Cool LG, Forschler BT, et al. 2001. Correspondence of soldier defense secretion mixtures with cuticular hydrocarbon phenotypes for chemotaxonomy of the termite genus *Reticulitermes* in North America. J. Chem. Ecol. 27:1449–1479. https://doi.org/10.1023/a:1010325511844

Nelson LJ, Cool LG, Solek CW, et al. 2008. Cuticular hydrocarbons and soldier defense secretions of *Reticulitermes* in southern California: a critical analysis of the taxonomy of the genus in North America. J. Chem. Ecol. 34:1452–1475. https://doi.org/10.1007/s10886-008-9548-6

Nelson LJ, Hamud SM, Baldwin JA, et al. 2022. Consistency of cuticular hydrocarbon mixtures of five *Reticulitermes* (Blattodea: Rhinotermitidae) taxa from northern California: Similarity among colonies and seasonal variation. J. Econ. Entomol. 116:209–222. https://doi.org/10.1093/jee/toac179

Nutting WL. 1990. Insecta, isoptera. In Dindal DL editor. Soil biology guide. Wiley. p. 997–1032.

Oksanen J, Simpson GL, Blanchet FG, et al. 2024. vegan: community ecology package. https://CRAN.R-project.org/package=vegan

Padial JM, Miralles A, De la Riva I, et al. 2010. The integrative future of taxonomy. Front. Zool. 7:16. https://doi.org/10.1186/1742-9994-7-16

Paradis E, Schliep K. 2019. ape 5.0: an environment for modern phylogenetics and evolutionary analyses in R. Bioinformatics 35:526–528. https://doi.org/10.1093/bioinformatics/bty633

Peakall R, Smouse PE. 2006. genalex 6: genetic analysis in Excel. Population genetic software for teaching and research. Mol. Ecol. Notes 6:288–295. https://doi.org/10.1111/j.1471-8286.2005.01155.x

Pickens AL. 1932. Distribution and life histories of the species of *Reticulitermes* Holmgren in California; a study of the subterranean termites with reference to (1) zoology, and (2) life histories [Doctoral Thesis]. University of California.

Pickens AL. 1934. The biology and economic significance of the western subterranean termite, *Reticulitermes hesperus*. In: Kofoid CA, Light SF, Horner AC, Randall M, et al. editors. Termites and termite control. 2nd ed. Revised. University of California Press. p. 157–183.

Pritchard JK, Stephens M, Donnelly P. 2000. Inference of population structure using multilocus genotype data. Genetics 155:945–959. https://doi.org/10.1093/genetics/155.2.945

Puechmaille SJ. 2016. The program structure does not reliably recover the correct population structure when sampling is uneven: subsampling and new estimators alleviate the problem. Mol. Ecol. Resour. 16:608–627. https://doi.org/10.1111/1755-0998.12512

R Core Team. 2024. R: A Language and Environment for Statistical Computing. Available from https://www.R-project.org/

Ratnasingham S, Hebert PDN. 2013. A DNA-based registry for all animal species: the barcode index number (BIN) system. PLoS One 8:e66213. https://doi.org/10.1371/journal.pone.0066213

Robinson JW. 1989. The San Bernardinos. The mountain country from Cajon Pass to Oak Glen. Two centuries of changing use. Big Santa Anita Historical Society.

Rosser N, Seixas F, Queste LM, et al. 2024. Hybrid speciation driven by multilocus introgression of ecological traits. Nature 628:811–817. https://doi.org/10.1038/s41586-024-07263-w

Rust MK, Saran RK. 2006. Toxicity, repellency, and transfer of chlorfenapyr against western subterranean termites (Isoptera: Rhinotermitidae). J. Econ. Entomol. 99:864–872. https://doi.org/10.1603/0022-0493-99.3.864

Rust MK, Saran RK. 2008. Toxicity, repellency, and effects of acetamiprid on western subterranean termite (Isoptera: Rhinotermitidae). J. Econ. Entomol. 101:1360–1366. https://doi.org/10.1603/0022-0493(2008)101[1360:traeoa]2.0.co;2

Saran RK, Rust MK. 2007. Toxicity, uptake, and transfer efficiency of fipronil in western subterranean termite (Isoptera: Rhinotermitidae). J. Econ. Entomol. 100:495–508. https://doi.org/10.1603/0022-0493(2007)100[495:tuateo]2.0.co;2

Scheffrahn RH, Su N-Y, Su N-Y. 1994. Keys to soldier and winged termites (Isoptera) of Florida. Fla. Entomol. 77:460–474. https://doi.org/10.2307/3495700

Simon C, Frati F, Beckenbach A, et al. 1994. Evolution, weighting, and phylogenetic utility of mitochondrial gene sequences and a compilation of conserved polymerase chain reaction primers. Ann. Entomol. Soc. Am. 87:651–701. https://doi.org/10.1093/aesa/87.6.651

Singhal S, Hoskin CJ, Couper P, et al. 2018. A framework for resolving cryptic species: a case study from the lizards of the Australian wet tropics. Syst. Biol. 67:1061–1075. https://doi.org/10.1093/sysbio/syy026

Snyder TE. 1949. Catalog of the termites (Isoptera) of the world. Smithsonian Miscellaneous Collections 112:1–490.

Snyder TE. 1954. Order Isoptera. The termites of the United States and Canada. National Pest Control Association. p. 64.

Su N-Y, Lee C-Y. 2023. Biology and management of the Formosan subterranean termite and related species. CABI. 427 p. https://play.google.com/store/books/details?id=ZP7rEAAAQBAJ

Su N-Y, Ye W, Ripa R, et al. 2006. Identification of Chilean *Reticulitermes* (Isoptera: Rhinotermitidae) inferred from three mitochondrial gene DNA sequences and soldier morphology. Ann. Entomol. Soc. Am. 99:352–363. https://doi.org/10.1603/0013-8746(2006)099[0352:IOCRIR]2.0.CO;2

Sutherland AM, Hubble C, Barber M. 2022. Installation season may significantly impact time required for subterranean termites to find and feed on in-ground baits. Insects 13:445. https://doi.org/10.3390/insects13050445

Szalanski AL, Austin JW, Mckern J, et al. 2006. Genetic evidence for a new subterranean termite species (Isoptera: Rhinotermitidae) from western United States and Canada. Fla. Entomol. 89:299–304. https://doi.org/10.1653/0015-4040(2006)89[299:gefans]2.0.co;2. http://www.jstor.org/stable/4092424

Tamura K, Stecher G, Kumar S. 2021. MEGA11: Molecular evolutionary genetics analysis version 11. Mol. Biol. Evol. 38:3022–3027. https://doi.org/10.1093/molbev/msab120

Tripodi AD, Austin JW, Szalanski AL, et al. 2006. Phylogeography of *Reticulitermes* termites (Isoptera: Rhinotermitidae) in California inferred from mitochondrial DNA sequences. Ann. Entomol. Soc. Am. 99:697–706. https://doi.org/10.1603/0013-8746(2006)99[697:portir]2.0.co;2

Tseng S-P, Nelson LJ, Hubble CW, et al. 2023. Phylogenetic analyses of *Reticulitermes* (Blattodea: Rhinotermitidae) from California and other western states: multiple genes confirm undescribed species identified by cuticular hydrocarbons. J. Econ. Entomol. 116:2135–2145. https://doi.org/10.1093/jee/toad182

Vargo EL. 2000. Polymorphism at trinucleotide microsatellite loci in the subterranean termite *Reticulitermes flavipes*. Mol. Ecol. 9:817–820. https://doi.org/10.1046/j.1365-294x.2000.00915.x

Wang M, Hellemans S, Šobotník J, et al. 2022. Phylogeny, biogeography and classification of Teletisoptera (Blattaria: Isoptera). Syst. Entomol. 47:581–590. https://doi.org/10.1111/syen.12548

Wickham H. 2016. Ggplot2: elegant graphics for data analysis. 2nd ed. Springer International Publishing (Use R!). p. 260 https://doi.org/10.1007/978-3-319-24277-4

Wu J, Xu H, Hassan A, et al. 2019. Interspecific hybridization between the two sympatric termite *Reticulitermes* species under laboratory conditions. Insects 11:14. https://doi.org/10.3390/insects11010014